phys. stat. sol. (a) **179**, 311 (2000)

Subject classification: 61.10.Dp; 61.72.Bb; 61.72.Dd; S5

Application of the Statistical Dynamical Theory of X-Ray Diffraction to Calculation of the HOPG Echelon-Monochromator Parameters

YA. I. NESTERETS (a), V. I. PUNEGOV (a), I. V. PIRSHIN (b), A. G. TOURYANSKI (b), A. V. VINOGRADOV (b), E. FÖRSTER (c), and S. G. PODOROV (c)

(a) Syktyvkar State University, Oktyabrskii prospect 55, 167001 Syktyvkar, Russia

(b) P. N. Lebedev Physical Institute, Russian Academy of Sciences, Leninskii prospect 53, 117324 Moscow A-333, Russia

(c) X-Ray Optics Group, Institute of Optics and Quantum Electronics, Friedrich Schiller University Jena, Max-Wien-Platz 1, D-07743 Jena, Germany

(Received November 2, 1999; in revised form February 10, 2000)

The statistical theory of X-ray diffraction and a mosaic crystal model are used to calculate the reflection and transmission factors for a row of pyrolytic graphite plates (echelon-monochromator). Experimental angular dependencies of reflection and transmission factors are compared with theoretical results. The data of reflection and transmission factors for both CuK_α- and CuK_β-lines depending on thickness of plates are given. The thickness of graphite plates for which the efficiency of the echelon-monochromator is optimal is determined.

1. Introduction

Highly Oriented Pyrolitic Graphite (HOPG) is widely used as a broadband filter of primary polychromatic radiation [1 to 3] and for focusing divergent monochromatic beams, thanks to its ability to preserve the orientation of the *c*-axis of crystalline blocks normal to the surface for samples grown on both flat and strongly curved substrates [4 to 7].

In a recent paper [7] the design of an X-ray echelon-monochromator is described, the basic elements of which are three semi-transparent HOPG plates. The overall performance of the given device depends on structural characteristics of HOPG and the plate thickness. In the present paper, the theoretical analysis and calculation of reflection and transmission factors (R and T, respectively) for real crystalline plates of pyrolytic graphite is made to explain the experimental results.

We shall also consider a simple echelon structure, consisting of a single semi-transparent and an opaque HOPG plate, which has been successfully used in X-ray reflectometers for multilayer structure investigations [8]. In this measurement scheme, two characteristic lines are simultaneously selected by the HOPG plates and registered in two counting channels. It will be shown that for the mentioned arrangement the factors T and R may be predicted and for samples with a given structure perfection any predetermined ratio of intensities for selected lines may be achieved by proper choice of the semi-transparent plate thickness.

2. Theory

The theoretical consideration of X-ray diffraction in a mosaic crystal of pyrolytic graphite is carried out on the basis of the statistical dynamical diffraction theory [9, 10].

For quantitative calculation of X-ray diffraction on a plate of pyrolytic graphite the model of a mosaic crystal is used. Following Darwin's theory [11], we assume the crystal to consist of a large number of crystalline blocks misoriented by a random angle α and shifted randomly with respect to each other (Fig. 1). The origin of coordinates is chosen to be in the centre of the block with axis z directed perpendicularly to a surface deep inside the crystal, and axes x and y are along the surface of the crystal in the plane of diffraction and perpendicularly to it, respectively. The turn of the mosaic block by an angle α around the y-axis causes a displacement of an arbitrary point (x, z) of the block by the vector $\delta\mathbf{u}$, whose components in the plane of diffraction under condition $\alpha \ll 1$ are: $u_x = \alpha z$ and $u_z = -\alpha x$. We restrict ourselves to the case of symmetric Bragg diffraction assuming the reciprocal lattice vector $\mathbf{h}$ of the reflecting planes to be perpendicular to the surface of the sample. In this case the atomic displacement function has the form:

$$\mathbf{h}\,\delta\mathbf{u}(x, z) = -h\,\delta u_z = hx\alpha\,.$$

In the statistical dynamical diffraction theory the angular distribution of incoherent (diffuse) intensity from a crystal with defects is defined by a correlation length

$$\tau(\Delta\theta) = \int_0^\infty \mathrm{d}\xi\, \exp\,(i\eta\xi)\, g(\xi)\,,$$

where the angular variable η is proportional to the deviation $\Delta\theta$ from the kinematical Bragg angle θ_B [12],

$$g(\xi) = \left(\langle \exp\,(-i\mathbf{h}[\delta\mathbf{u}(\xi) - \delta\mathbf{u}(0)])\rangle - E^2\right)/(1 - E^2)$$

is a correlation function and $E = \langle \exp\,(-i\mathbf{h}\cdot\delta\mathbf{u})\rangle$ is the static Debye-Waller factor. Brackets $\langle \ldots \rangle$ denote the result of statistical averaging.

In the following, we assume the relative displacement of the blocks to be comparable to the X-ray wavelength λ. This allows the phase correlation of waves scattered by different blocks to be ignored, i.e. to consider the mosaic crystal as an array of independently scattering ideal blocks. For such a crystal model the static Debye-Waller factor is

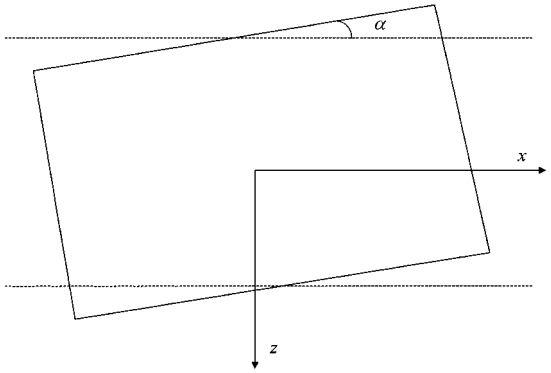

Fig. 1. Model of the crystalline block

equal to zero ($E = 0$) and the correlation function takes the form

$$g(\xi) = p(\xi) \int_{-\infty}^{\infty} \mathrm{d}\alpha \; W(\alpha) \exp\left(iB\alpha\xi\right), \tag{1}$$

where $B = 4\pi \cos\theta_B/\lambda$; $p(\xi)$ is the probability that two points lying on the reflected beam, having a separate ξ along the z-axis, belong to the same block; $W(\alpha)$ is the block misorientation distribution function. Hereinafter, the Gaussian distribution with half width at half maximum Δ_m is used, i.e.

$$W(\alpha) = \sqrt{\frac{\ln 2}{\pi}} \frac{1}{\Delta_m} \exp\left(-\ln 2 \frac{\alpha^2}{\Delta_m^2}\right).$$

Taking this into account, the correlation function and correlation length are written respectively as

$$g(\xi) = \exp\left(-A^2\xi^2\right) p(\xi); \qquad A = \frac{\Delta_m B}{2\sqrt{\ln 2}}$$

and

$$\tau(\Delta\theta) = \int_0^{\infty} \mathrm{d}\xi \exp\left(i\eta\xi\right) \exp\left(-A^2\xi^2\right) p(\xi). \tag{2}$$

The explicit expression for the correlation length is dependent on the specific probability function $p(\xi)$ determined by the shape and size of the mosaic blocks. We consider the crystal to consist of mosaic blocks in the form of plates which thickness l much less than their lateral size. In this case the probability function takes the form

$$p(\xi) = \begin{cases} 1 - \xi/l; & \xi \le l, \\ 0; & \xi > l. \end{cases}$$

The explicit expression for the correlation length is then

$$\tau(\Delta\theta) = \frac{1}{A^2 l} \left\{ \frac{\sqrt{\pi}}{2} \left[i \frac{\eta}{2A} - Al \right] \exp\left(-\frac{\eta^2}{4A^2}\right) \left[\mathrm{erf}\left(i \frac{\eta}{2A} - Al \right) - \mathrm{erf}\left(i \frac{\eta}{2A} \right) \right] + \frac{1}{2} \left[\exp\left(i\eta l - A^2 l^2\right) - 1 \right] \right\}. \tag{3}$$

The system of equations for diffuse intensities in the statistical theory [10] are written (assuming as stated above that for our mosaic crystal the static Debye-Waller factor is equal to zero, $E = 0$)

$$\begin{cases} \dfrac{\mathrm{d}I_0^d}{\mathrm{d}z} = -\mu_0 I_0^d + \varkappa_{-h} I_h^d, \\ -\dfrac{\mathrm{d}I_h^d}{\mathrm{d}z} = -\mu_h I_h^d + \varkappa_h (I_0^d + I_0^c), \end{cases} \tag{4}$$

where $\mu_{0,h} = \mu/\gamma_{0,h} + 2\,\mathrm{Re}\,(\sigma_h\sigma_{-h}\tau)$, $\varkappa_{\pm h} = 2|\sigma_{\pm h}|\,2\,\mathrm{Re}\,(\tau)$, μ is the linear absorption coefficient, $\sigma_{\pm h} = \pi\chi_{\pm h} C/\lambda\gamma_{h,0}$, $\chi_{\pm h}$ are the h-th and $(-h)$-th Fourier components of the crystal susceptibility, C is the polarization factor ($C = 1$ for the σ-component and

$C = \cos 2\theta_B$ for the π-component), $\gamma_{0,h}$ are the direction cosines of the incident and diffracted waves. Hereafter we use designations introduced in [12].

In the absence of coherently scattered intensity, the equation for coherent transmitted intensity takes the form

$$\frac{dI_0^c}{dz} = -\mu_0 I_0^c . \tag{5}$$

Summing the first equation in (4) and equation (5), the equation for total transmitted intensity I_0 is found

$$\frac{dI_0}{dz} = -\mu_0 I_0 + \varkappa_{-h} I_h^d . \tag{6}$$

Eq. (6), together with the second equation in (4), can be written as

$$\frac{dI_h^d}{dz} = \mu_h I_h^d - \varkappa_h I_0 , \tag{7}$$

form a pair of differential equations for calculation of the reflection and transmission coefficients of our mosaic crystal. In the Bragg case the boundary conditions for a parallel plate of thickness L are

$$I_0(z=0) = 1 , \qquad I_h^d(z=L) = 0 .$$

For the symmetrical diffraction case we have $\mu_h = \mu_0$ and the general solution of the system (6), (7) is written down as follows:

$$I_h^d(z) = C_1 \sin \Lambda z + C_2 \cos \Lambda z , \qquad I_0(z) = C_3 \sin \Lambda z + C_4 \cos \Lambda z ,$$

where $\Lambda = (\varkappa_h \varkappa_{-h} - \mu_0^2)^{1/2}$.

Coefficients $C_{1,2,3,4}$ are related by the following expressions:

$$C_3 = \frac{\mu_0 C_1 + \Lambda C_2}{\varkappa_h} , \qquad C_4 = \frac{\mu_0 C_2 - \Lambda C_1}{\varkappa_h} .$$

Using the boundary conditions, the explicit forms for C_1 and C_2 are found:

$$C_1 = \frac{-\varkappa_h \cos \Lambda L}{\Lambda \cos \Lambda L + \mu_0 \sin \Lambda L} , \qquad C_2 = -C_1 \operatorname{tg} \Lambda L = \frac{\varkappa_h \sin \Lambda L}{\Lambda \cos \Lambda L + \mu_0 \sin \Lambda L} .$$

Thus, the solutions for reflected and transmitted intensities have the form

$$I_h^d(z) = \frac{\varkappa_h \sin \Lambda (L-z)}{\Lambda \cos \Lambda L + \mu_0 \sin \Lambda L} , \qquad I_0(z) = \frac{\mu_0 \sin \Lambda (L-z) + \Lambda \cos \Lambda (L-z)}{\Lambda \cos \Lambda L + \mu_0 \sin \Lambda L} .$$

Hence the reflection and transmission coefficients for a mosaic crystal in symmetrical geometry are

$$R = I_h^d(0) = \frac{\varkappa_h \sin \Lambda L}{\Lambda \cos \Lambda L + \mu_0 \sin \Lambda L} , \qquad T = I_0(L) = \frac{\Lambda}{\Lambda \cos \Lambda L + \mu_0 \sin \Lambda L} . \tag{8}$$

The solutions (8) form the basis of a numerical algorithm which accounts for reflection by mosaic structures. It is follows from (8) that the reflection and transmission coefficients depend on the plate thickness L, mosaic block parameters l and Δ_m (via correlation length τ) and on the incident wave polarization (via $\varkappa_h$ and μ_0).

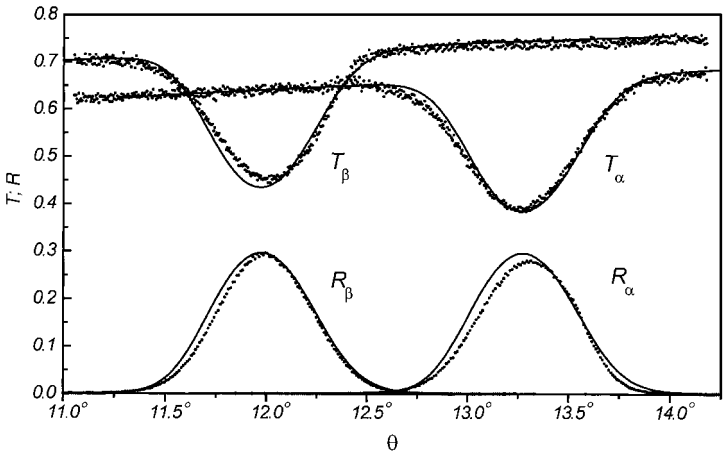

Fig. 2. The experimental and theoretical angular distributions of reflection and transmission factors of the HOPG plate for CuK_α and CuK_β radiation ($\Delta_m = 900''$, $l = 0.1$ μm, $L = 103$ μm)

3. Experimental and Numerical Results

In Fig. 2, the experimental angular distributions of reflection and transmission factors of the HOPG plate for CuK_α and CuK_β radiation using the double crystal diffractometer described in [7] are shown. Since the structural characteristics of pyrolytic graphite were not investigated in [7], the numerical simulation of rocking curves was performed. The best agreement of experimental and theoretical results was achieved using the following graphite plate parameters: thickness of the plate is $L = 103$ μm, thickness of the single mosaic block is $l = 0.1$ μm, half width at half maximum of the block misorientation distribution function is equal to $\Delta_m = 900''$. In Fig. 2 the corresponding theoretical curves (solid lines) calculated using formulae (8) and the above graphite plate parameters are shown. We have investigated a number of HOPG plates of various thickness and have obtained parameters of mosaic blocks (i.e. block thickness l and misorientation spread Δ_m) to be almost the same.

Fig. 3 shows the scheme of the pyrolytic graphite echelon-monochromator which selects the K_α- and K_β-line of the X-ray spectrum. In the scheme 1, the first plate of HOPG is thinner and reflects the K_α-line radiation, whereas the second thick plate reflects radiation of the K_β-line. In scheme 2 the reflection sequence for the considered lines is reversed.

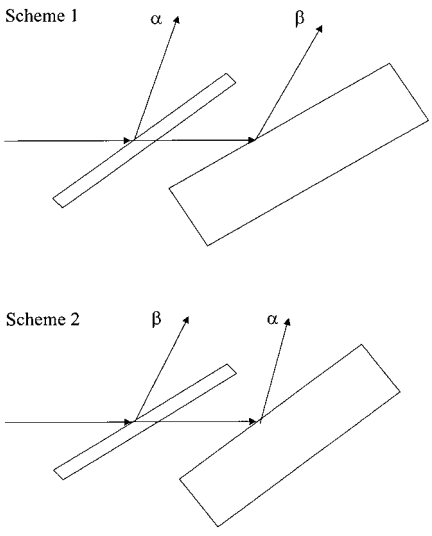

Fig. 3. Schemes of the pyrographite echelon-monochromators

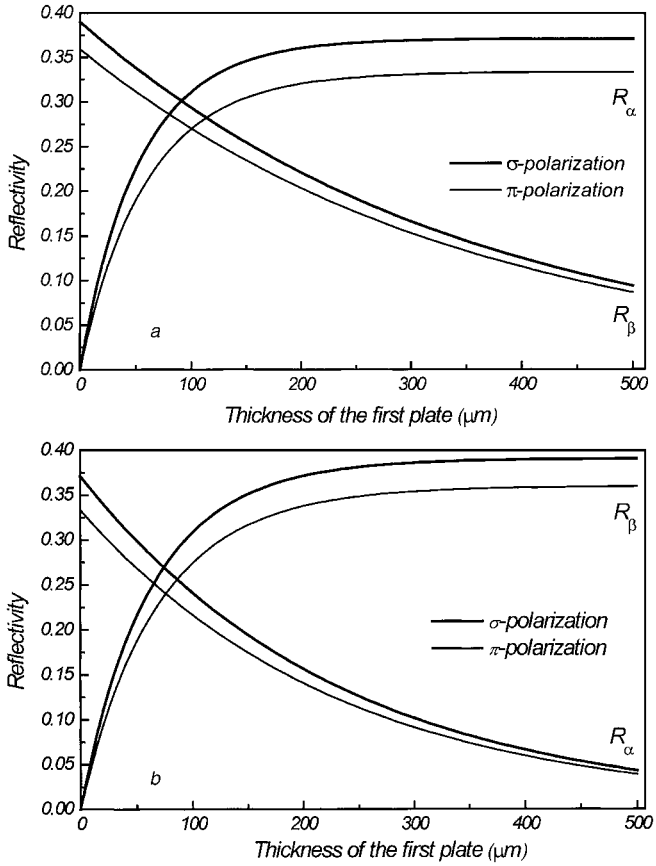

Fig. 4. Calculated dependence of reflectance coefficients for CuK_α and CuK_β radiation vs. thickness for a) Scheme 1 and b) Scheme 2 shown in Fig. 3

Using the mosaic spread parameters obtained from the analysis of experimental curves in Fig. 4, the calculated dependence of reflectance coefficients for CuK_α and CuK_β radiation versus thickness of the first plate of monochromator for both schemes are shown. The thickness of the second plate is constant and equal to 500 μm. The symmetrical (002)-reflection was considered. According to scheme 1, the first plate is set in position satisfying the Bragg condition for α-line ($\theta_{B,\alpha} = 13.278^\circ$) whereas the second is that for β-line ($\theta_{B,\beta} = 11.978^\circ$). Let $R_{i,j}$ and $T_{i,j}$ designate the reflection and transmission coefficients of the first plate for radiation of the i-th line satisfying the Bragg condition for j-th line and $R^\infty_{i,j}$ designate these coefficients for the second semi-infinite plate. Hence the reflectance coefficients for α- and β-line in scheme 1 and 2 are written, respectively, as

$$\begin{cases} R_\alpha^{(1)} = R_{\alpha,\alpha}\,, & R_\beta^{(1)} = T_{\beta,\alpha} R^\infty_{\beta,\beta}\,, \\ R_\alpha^{(2)} = T_{\alpha,\beta} R^\infty_{\alpha,\alpha}\,, & R_\beta^{(2)} = R_{\beta,\beta}\,. \end{cases} \tag{9}$$

It follows from Fig. 4a that equal factors of reflection in the first scheme of monochromator with the above structural characteristics of pyrolytic graphite are achieved at

90 μm thickness of the first plate for σ-polarization, 100 μm for π-polarization and at 75 μm in the second scheme for both states of polarization. As the first scheme on average (for non-polarized radiation) gives a reflection factor about 0.28 and the second 0.25, the utilization of the first scheme is preferred from this point of view.

The intensities of CuK_α- and CuK_β-lines emitted by an X-ray tube differ by 5. The use of the first scheme gives equality of reflected intensities at approximately 10 μm thickness of the first plate which is difficult to realize technologically. The second scheme provides equality of reflected intensities at a more reasonable 460 μm thickness of the first crystal, with reflection factor about 0.04.

It is necessary to emphasize that Fig. 4 has a more abundant content. On the one hand it allows to calculate the reflection factors of the CuK_α- and CuK_β-lines for an arbitrary thickness of the first plate and, consequently, the intensity ratio of the CuK_α- and CuK_β-components of the radiation. On the over hand it is possible to estimate using Fig. 4 the thickness of the first plate of monochromator to obtain the necessary ratio of the reflected intensities of the CuK_α- and CuK_β-components of X-ray radiation.

4. Concluding Remarks

It has been demonstrated that calculations of transparency and reflectivity characteristics of single HOPG plates and an echelon arrangement with the use of statistical dynamical theory of X-ray diffraction gives a satisfactory explanation of the observed experimental results. The small discrepancies could be due to variations of the mosaic spread parameter and plate thickness along the length of the irradiated area which is ≈ 1 cm. This is confirmed by measurements obtained by linear scanning with a 30 mm diaphragm placed near the HOPG plate. The approach may be also used to predict transparency and reflectivity for any predetermined number of semitransparent plates and calculate other parameters of the echelon, for instance, its bandpass when all plates are tuned to one spectral line.

Acknowledgements The authors are grateful to the International Association for cooperation of scientists of CIS and Western Europe countries (grant INTAS-96-0128), to the Education Ministry of the Russian (grant N 97-0-7.2-116) and to Syktyvkar State University (within university grant) for financial support.

References

[1] D. H. Bilderback, Nucl. Instrum. Methods **195**, 67 (1982).
[2] A. K. Freund, Proc. SPIE **1740**, 58 (1992).
[3] A. K. Freund, Nucl. Instrum. Methods A **266**, 461 (1988).
[4] A. A. Antonov, V. B. Baryshev, I. G. Grigoryeva, G. N. Kulipanov, and N. N. Shirkov, Nucl. Instrum. Methods A **308**, 442 (1991).
[5] G. Pareschi, F. Frontera, P. Chiara, G. Ferrara, and E. Costa, Proc. SPIE **3113**, 275 (1997).
[6] B. Beckhoff, B. Kanngiesser, and W. Malzer, Proc. SPIE **2859**, 190 (1996).
[7] A. G. Touryanski and I. V. Pirshin, Instruments and Experimental Techniques **41**, No. 5, 118 (1998).
[8] A. G. Touryanski, A. V. Vinogradov, and I. V. Pirshin, Instruments and Experimental Techniques **42**, No. 1, 94 (1999).
[9] N. Kato, Acta Cryst. A **32**, 453, 458 (1976).
[10] V. A. Bushuev, Soviet Phys.–Crystallogr. **34**, 163 (1989).
[11] C. G. Darwin, Phil. Mag. **43**, 800 (1922).
[12] V. I. Punegov, phys. stat. sol. (a) **136**, 9 (1993).